

# PDE-CONSTRAINED OPTIMIZATION OF TIME-DEPENDENT 3D ELECTROMAGNETIC INDUCTION HEATING BY ALTERNATING VOLTAGES

FREDI TRÖLTZSCH\* AND IRWIN YOUSEPT\*

**Abstract.** This paper is concerned with a PDE-constrained optimization problem of induction heating, where the state equations consist of 3D time-dependent heat equations coupled with 3D time-harmonic eddy current equations. The control parameters are given by finite real numbers representing applied alternating voltages which enter the eddy current equations via impressed current. The optimization problem is to find optimal voltages so that, under certain constraints on the voltages and the temperature, a desired temperature can be optimally achieved. As there are finitely many control parameters but the state constraint has to be satisfied in an infinite number of points, the problem belongs to a class of semi-infinite programming problems. We present a rigorous analysis of the optimization problem and a numerical strategy based on our theoretical result.

**Key words.** PDE-constrained optimization, electromagnetic induction heating, time-variant heat equations, time-harmonic eddy current equations, pointwise state constraints, semi-infinite programming, optimality conditions.

**AMS subject classifications.** 49J20, 78A25, 78A30, 35K40, 90C48.

**1. Introduction.** Electromagnetic induction heating is a well-known technique used widely in many industrial applications to heat electrically conducting materials such as metals. A typical induction heating system involves at least the following two main parts: a set of induction coils connected to a power supply and an electrically conducting workpiece. The power supply induces a high-frequency alternating current (AC) in the induction coil which in turn generates a magnetic field. Then, the resistance to the eddy current in the workpiece induces heat (cf. [15]). The underlying mathematical model for electromagnetic induction heating consists of coupled PDEs involving a nonlinear heat equation and Maxwell's equations. The analysis and numerical modeling of induction heating have been studied by many authors. We refer to Bossavit and Rodrigues [5], Clain and Touzani [8], Clain, Rappaz, Swierkosz, and Touzani [7], Hömberg [12, 13], Parietti and Rappaz [19, 20], and Rappaz and Swierkosz [21].

For our mathematical model, we consider a bounded domain  $\mathcal{D} \subset \mathbb{R}^3$  containing a set of induction coils  $\bar{\mathcal{I}} \subset \mathcal{D}$  and a workpiece  $\bar{\Omega} \subset \mathcal{D}$  satisfying  $\bar{\mathcal{I}} \cap \bar{\Omega} = \emptyset$ . The region  $\mathcal{D} \setminus (\bar{\Omega} \cup \bar{\mathcal{I}})$  represents the surrounding air (see Figure 1.2 for an exemplary geometry). The precise assumptions on geometry and given data will be specified later. As a simplified model for induction heating in the workpiece  $\Omega$ , we consider the following 3D parabolic initial-boundary value problem:

$$(1.1) \quad \begin{cases} \frac{\partial y}{\partial t} - \operatorname{div}(\alpha \nabla y) = \sigma \left| \frac{\partial \mathcal{A}}{\partial t} \right|^2 \tau & \text{in } Q := \Omega \times (0, T) \\ \nu \cdot \alpha \nabla y = 0 & \text{in } \Sigma := \partial\Omega \times (0, T) \\ y(\cdot, 0) = y_0 & \text{in } \Omega. \end{cases}$$

Here,  $y = y(x, t)$  denotes the temperature distribution,  $\mathcal{A} = \mathcal{A}(x, t)$  the magnetic vector potential,  $\nu = \nu(x)$  the outward unit normal at  $x \in \partial\Omega$ ,  $\alpha = \alpha(x)$  the thermal diffusivity,  $\sigma = \sigma(x)$  the electrical conductivity and  $y_0 = y_0(x)$  initial data. The heat source  $\sigma \left| \frac{\partial \mathcal{A}}{\partial t} \right|^2$  arises from the Joule heating

---

\*Institut für Mathematik, Technische Universität Berlin, D-10623 Berlin, Str. des 17. Juni 136, Germany (troeltzsch@math.tu-berlin.de, yousept@math.tu-berlin.de). The authors acknowledge support through DFG Research Center MATHEON "Mathematics for Key Technologies" (FZT 86) in Berlin.

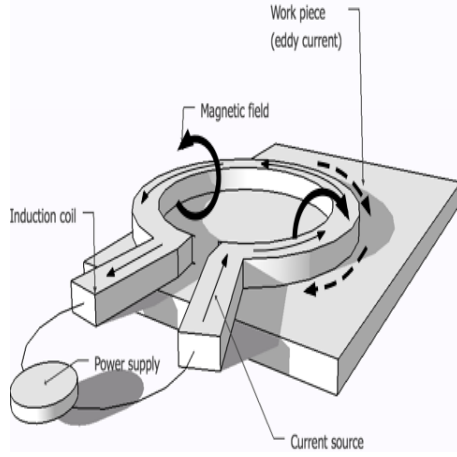


FIG. 1.1. Illustration of electromagnetic induction heating.

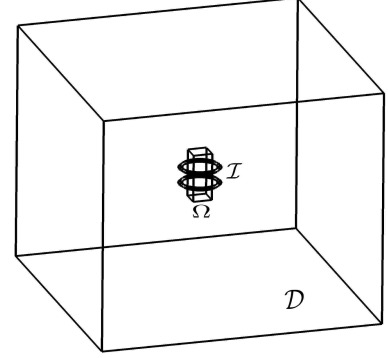


FIG. 1.2. Exemplary 3D geometry.

effect; see for instance [13]. Further,  $\tau$  is a function of time satisfying

$$(1.2) \quad \tau(t) = \begin{cases} 1 & \text{if } t \in [0, T_E] \\ 0 & \text{if } t \in (T_E, T], \end{cases}$$

with some  $T_E \in (0, T)$ . Thus, in the time interval  $(T_E, T]$ , the AC power supply is turned off.

The magnetic vector potential  $\mathcal{A}$  in (1.1) is given by the time harmonic ansatz

$$(1.3) \quad \mathcal{A}(x, t) = \Im(\mathcal{A}(x) \exp(i\omega t)),$$

with a fixed angular frequency  $\omega > 0$ , and the complex-valued vector function  $\mathcal{A} : \mathcal{D} \rightarrow \mathbb{C}^3$  solves the following eddy current equations:

$$(1.4) \quad \begin{cases} \nabla \times (\mu^{-1} \nabla \times \mathcal{A}) + i\omega\sigma\mathcal{A} = j_g & \text{in } \mathcal{D} \\ \operatorname{div} \mathcal{A} = 0 & \text{in } \mathcal{D} \\ \mathcal{A} \times \nu = 0 & \text{on } \partial\mathcal{D}. \end{cases}$$

Here,  $j_g = j_g(x)$  is the impressed alternating current,  $\mu = \mu(x)$  the magnetic permeability, and  $i$  the imaginary unit. In general, the eddy current equations (1.4) need to be posed in the whole space  $\mathbb{R}^3$  since they involve electromagnetic fields that cannot be easily measured on boundaries of given bounded domains. However, the parts of the electromagnetic fields sufficiently far from the conductors  $\bar{\mathcal{I}}$  and  $\bar{\Omega}$  are rather negligible. Therefore, to simplify the problem, we suppose that the boundary  $\partial\mathcal{D}$  is far from  $\bar{\mathcal{I}}$  and  $\bar{\Omega}$  and consider the eddy current model in a large "hold all" domain  $\mathcal{D}$  along with a standard electric boundary condition (cf. the monograph by Alonso and Valli [1]).

We explain now how  $j_g$  in our situation looks like. Let  $\mathcal{I} = \mathcal{I}_1 \cup \dots \cup \mathcal{I}_n$ , with  $n \in \mathbb{N}$ , satisfying  $\bar{\mathcal{I}}_i \cap \bar{\mathcal{I}}_j = \emptyset$  for  $i \neq j$ . For each  $j \in \{1, \dots, n\}$ ,  $\mathcal{I}_j$  is a torus, i.e., there exist real numbers  $d_{j,1}, d_{j,2} > 0$  such that

$$\mathcal{I}_j = \left\{ z_j + \begin{pmatrix} (d_{j,1} + s \cos \eta) \cos \theta \\ (d_{j,1} + s \cos \eta) \sin \theta \\ s \sin \eta \end{pmatrix} : s \in [0, d_{j,2}], \eta, \theta \in [0, 2\pi] \right\}, \quad z_j \in \mathbb{R}^3.$$

The alternating voltages  $u_j$  in the induction coils  $\mathcal{I}_j$  ( $j = 1, \dots, n$ ) are our controls. We assume that, in each coil  $\mathcal{I}_j$ , the voltage  $u_j \in \mathbb{R}$  can be kept constant, and there is no coupling effect between the voltages. Then, the current  $j_g$  in each induction coil  $\mathcal{I}_j$  is obtained from Ohm's law by the associated electrical resistance of  $\mathcal{I}_j$  as the voltage  $u_j$  is applied. Summarizing, the impressed alternating current  $j_g$  is given by the ansatz

$$(1.5) \quad j_g(x) = \sum_{j=1}^n u_j \mathcal{J}_j(x),$$

where

$$(1.6) \quad \mathcal{J}_j(x) = \begin{cases} 1/R_j(-x_3/\sqrt{x_1^2+x_3^2}, 0, x_1/\sqrt{x_1^2+x_3^2})^T & \text{if } x \in \bar{\mathcal{I}}_j \\ 0 & \text{if } x \notin \bar{\mathcal{I}}_j. \end{cases}$$

Here,  $R_j$  denotes the electrical resistance of  $\mathcal{I}_j$  which is assumed to be a positive constant. Note that the construction (1.5) implies in particular that

$$(1.7) \quad \operatorname{div} j_g = 0 \text{ in } \mathcal{I}, \quad \nu \cdot j_g = 0 \text{ on } \partial\mathcal{I}.$$

The choice of  $\mathcal{J}_j$  is not restricted to (1.6). Our analysis is also true for all vector fields  $\mathcal{J}_j$  satisfying  $\operatorname{div} \mathcal{J}_j = 0$  in  $\mathcal{I}$  and  $\nu \cdot \mathcal{J}_j = 0$  on  $\partial\mathcal{I}$  for all  $j = 1, \dots, n$ . Further, we should underline that the counteraction of the magnetic field on the current in the induction coils is included in this model. Our simplifying assumption concerns only the voltages in the coils.

In induction heating, the oscillatory period of the magnetic vector potential  $\mathcal{A}$  is significantly smaller than the diffusion time. Therefore, we approximate the Joule heat source  $\sigma \left| \frac{\partial \mathcal{A}}{\partial t} \right|^2$  by its average value over one period  $(0, 2\pi/\omega)$ , i.e., by

$$\frac{\omega}{2\pi} \int_0^{\frac{2\pi}{\omega}} \sigma \left| \frac{\partial \mathcal{A}}{\partial t}(x, t) \right|^2 dt \stackrel{(1.3)}{=} \frac{\sigma \omega^2}{2} |\mathcal{A}(x)|^2.$$

Our paper is concerned with an optimization problem of finding optimal voltages to achieve a desired temperature at the final time  $t = T$  under certain constraints on the voltages and the temperature. More precisely, we consider the following optimal control problem:

$$(P) \quad \min \frac{1}{2} \int_{\Omega} |y(x, T) - y_d(x)|^2 dx$$

subject to

$$(1.8a) \quad \begin{cases} \nabla \times (\mu^{-1} \nabla \times \mathcal{A}) + i\omega \sigma \mathcal{A} = \sum_{j=1}^n u_j \mathcal{J}_j & \text{in } \mathcal{D} \\ \operatorname{div} \mathcal{A} = 0 & \text{in } \mathcal{D} \\ \mathcal{A} \times \nu = 0 & \text{on } \partial\mathcal{D}, \end{cases}$$

$$(1.8b) \quad \begin{cases} \frac{\partial y}{\partial t} - \operatorname{div}(\alpha \nabla y) = \frac{\tau \sigma \omega^2}{2} |\mathcal{A}|^2 & \text{in } Q \\ \nu \cdot \alpha \nabla y = 0 & \text{in } \Sigma \\ y(\cdot, 0) = y_0 & \text{in } \Omega, \end{cases}$$

and to the following control- and state-constraints

$$\begin{aligned} (1.9a) \quad & u_a \leq u_j \leq u_b \quad \text{for all } j = 1, \dots, n, \\ (1.9b) \quad & y(x, t) \leq y_{\max} \quad \text{for almost all } (x, t) \in Q. \end{aligned}$$

In (P),  $y_d \in L^2(\Omega)$  is the desired temperature. The real lower and upper bounds  $u_a, u_b \in \mathbb{R}$  satisfy  $0 \leq u_a < u_b$  and represent the minimum and maximum voltage allowed for the induction heating. To avoid undesired damage or melting of the material  $\Omega$  during the heating process, it is particularly significant to include the pointwise state constraint (1.9b). Here,  $y_{\max} \in \mathbb{R}^+$  stands for the allowed maximum temperature which may not be exceeded during the heating process. Note that the optimal control problem (P) belongs to a class of semi-infinite programming problems (SIP) as it involves finitely many control parameters but the state constraint (1.9b) needs to be satisfied in an infinite number of points. Here we do not include a Tikhonov regularization term in the objective functional of (P). Let us also remark that our results remain true for the heat equations involving Dirichlet- or Robin-type boundary conditions instead of the homogeneous Neumann-type boundary condition. This causes only minor and obvious modifications.

In literature, there are some contributions towards the mathematical analysis and the numerical investigation of optimal control of induction heating problems. We mention Bodart et al. [3] concerning a numerical study in a two-dimensional setting without pointwise state constraints. We also refer to [9, 24] for the analysis of optimal control of 3D *stationary* induction heating problems (see also [25] for the numerical analysis of optimal control problems of Maxwell's equations). To our best knowledge, the mathematical analysis and the numerical treatment for optimal control of 3D induction heating problems with time-dependent temperature and pointwise state constraints have not been investigated in literature. The mathematical analysis and the numerical investigation of (P) represent therefore the main contributions of this paper.

To derive Karush-Kuhn-Tucker (KKT) type optimality conditions for (P), we need the continuity of the temperature. Due to the squared term in the right hand side of the parabolic equation in (1.8), this is not obvious. We show the continuity of the temperature by a recent parabolic regularity result of Griepentrog [10] (Lemma 3.2 and Theorem 3.3). Then, as a consequence of the continuity, KKT type optimality conditions for local optima of (P) can be established relying on a standard regularity assumption on the optimal solution. Furthermore, employing a superposition principle, we provide a simplified expression for the mapping  $u \mapsto y$ . Based on this expression, we obtain optimality conditions for (P), in a simplified form, which do not involve an adjoint state and reveal a more specific structural property for the Lagrange multiplier (Theorem 4.5). After investigating the first-order analysis of (P), we present a second-order sufficient optimality condition for a feasible control of (P) which ensures its local optimality. We close this paper by considering a specific test example and present our numerical strategy for solving this problem.

**2. General assumptions and notation.** Let us introduce the mathematical setting including the notation used throughout this paper. We denote by  $c$  a generic positive constant which can take different values on different occasions. If  $V$  is a linear normed function space, then we use the notation  $\|\cdot\|_V$  for a standard norm used in  $V$ . Furthermore, we set  $V^3 := V \times V \times V$ . The dual space of  $V$  is denoted by  $V^*$  and, for the associated duality pairing, we write  $\langle \cdot, \cdot \rangle_{V^*, V}$ . A continuous embedding of  $V$  in another linear normed function space  $Y$  is denoted by  $V \hookrightarrow Y$ . For the Fréchet derivative of a differentiable operator  $B : V \rightarrow Y$  at  $v \in V$  in the direction  $h \in V$ , we

write  $B'(v)h$ . We recall the curl- and div-spaces:

$$\begin{aligned} H(\text{curl}; \mathcal{D}) &:= \{K \in L^2(\mathcal{D}; \mathbb{C})^3 \mid \nabla \times K \in L^2(\mathcal{D}; \mathbb{C})^3\}, \\ H(\text{div}; \mathcal{D}) &:= \{K \in L^2(\mathcal{D}; \mathbb{C})^3 \mid \text{div} K \in L^2(\mathcal{D}; \mathbb{C})\}, \end{aligned}$$

where the curl-operator ( $\nabla \times \cdot$ ) and div-operator are understood in the distribution sense (cf. [2]). In the above definition,  $L^2(\mathcal{D}; \mathbb{C})$  denotes the space of complex-valued Lebesgue square-integrable functions defined on  $\mathcal{D}$ . For the solution of the parabolic problem, we use the space

$$W(0, T) = \left\{ y \in L^2(0, T; H^1(\Omega)) \mid \frac{\partial y}{\partial t} \in L^2(0, T; H^1(\Omega)^*) \right\};$$

see Lions and Magenes [14]. The space of regular Borel measures on the compact set  $\overline{Q}$  is denoted in this paper by  $\mathcal{M}(\overline{Q})$ . Based on the Riesz-Radon theorem, the dual space  $\mathcal{C}(\overline{Q})^*$  can be isometrically identified with  $\mathcal{M}(\overline{Q})$ . We further set

$$\mathcal{M}(\overline{Q})^+ = \left\{ \lambda \in \mathcal{M}(\overline{Q}) \mid \int_{\overline{Q}} y d\lambda \geq 0 \quad \forall y \in \mathcal{C}(\overline{Q}) \text{ with } y(x, t) \geq 0 \quad \forall (x, t) \in \overline{Q} \right\}.$$

We now state the mathematical assumptions on geometry and given data involved in (P):

ASSUMPTION 2.1 (General assumptions).

(i) We assume that  $\mathcal{D} \subset \mathbb{R}^3$  is a simply connected convex domain satisfying  $\overline{\Omega}, \overline{\mathcal{I}} \subset \mathcal{D}$ . The subdomain  $\Omega$  is assumed to be Lipschitz in the sense of Grisvard [11].

(ii) The initial temperature  $y_0$  is a continuous function satisfying  $0 \leq y_0(x) < y_{\max}$  for all  $x \in \overline{\Omega}$ . Further, we assume that  $\mu, \sigma \in L^\infty(\mathcal{D})$ , and  $\alpha \in L^\infty(\Omega)$  satisfy

$$(2.1) \quad \begin{cases} 0 < \mu_{\min} \leq \mu(x) \leq \mu_{\max} < \infty & \text{for a.a. } x \in \mathcal{D}, \\ 0 < \alpha_{\min} \leq \alpha(x) \leq \alpha_{\max} < \infty & \text{for a.a. } x \in \Omega, \\ 0 < \sigma_{\min} \leq \sigma(x) \leq \sigma_{\max} < \infty & \text{for a.a. } x \in \mathcal{I} \cup \Omega, \\ \sigma(x) = 0 & \text{for all } x \in \mathcal{D} \setminus \overline{(\mathcal{I} \cup \Omega)}. \end{cases}$$

Note that  $\sigma$  vanishes in the subset  $\mathcal{D} \setminus \overline{(\mathcal{I} \cup \Omega)}$  as it represents the air surrounding the conductors  $\Omega$  and  $\mathcal{I}$ , which is electrically nonconducting.

**3. Analysis of (P).** We start by introducing the Banach space

$$X = \left\{ K \in H(\text{curl}; \mathcal{D}) \cap H(\text{div}; \mathcal{D}) \mid \text{div} K = 0 \text{ in } \mathcal{D}, \quad K \times \nu = 0 \text{ on } \partial\mathcal{D} \right\},$$

which is endowed with the norm

$$\|\psi\|_X = \|\psi\|_{H(\text{curl}; \mathcal{D})} = (\|\psi\|_{L^2(\mathcal{D}; \mathbb{C})^3}^2 + \|\nabla \times \psi\|_{L^2(\mathcal{D}; \mathbb{C})^3}^2)^{\frac{1}{2}} \quad \forall \psi \in X.$$

DEFINITION 3.1. The pair  $(\mathcal{A}, y) \in X \times W(0, T)$  is called a (weak) solution to (1.8) if and only if  $y(0) = y_0$  and

$$(3.1a) \quad \int_{\mathcal{D}} (\mu^{-1} \nabla \times \mathcal{A}) \cdot (\nabla \times \overline{\psi}) dx + i\omega \int_{\mathcal{I} \cup \Omega} \sigma \mathcal{A} \cdot \overline{\psi} dx = \sum_{j=1}^n u_j \int_{\mathcal{I}_j} \mathcal{J}_j \cdot \overline{\psi} dx \quad \forall \psi \in X$$

$$(3.1b) \quad \int_0^T \left\langle \frac{\partial y}{\partial t}, \phi \right\rangle_{H^1(\Omega)^*, H^1(\Omega)} dt + \iint_Q \alpha \nabla y \cdot \nabla \phi dx dt = \iint_Q \frac{\tau \sigma \omega^2}{2} |\mathcal{A}|^2 \phi dx dt \quad \forall \phi \in W(0, T).$$

In other words:  $\mathcal{A}$  is a weak solution to (1.8a) and  $y$  is a weak solution of (1.8b) in the standard sense.

Notice that  $\bar{\psi}$  in (3.1a) denotes the complex conjugate of  $\psi$ . This should not lead to any confusion with the notation  $\bar{Q}, \bar{\Omega}, \bar{\mathcal{I}}$ , etc., which denotes the closure of these sets.

In the upcoming lemma, we provide a parabolic regularity result. Here, instead of  $\Omega \subset \mathcal{D} \subset \mathbb{R}^3$ , we consider a general bounded Lipschitz-domain  $\Omega$  in  $\mathbb{R}^N$  with  $N \in \mathbb{N}$ . For the proof of this lemma, we refer to [10, Theorem 6.8] or [22, Lemma 7.12] (cf. also Casas [6]).

LEMMA 3.2. *Let  $\Omega \in \mathbb{R}^N$ ,  $N \in \mathbb{N}$ , be a bounded Lipschitz-domain in the sense of Grisvard [11] and let  $v \in L^r(Q)$  with  $r > \frac{N}{2} + 1$ . Then, the weak solution  $z \in W(0, T)$  to the linear parabolic initial-boundary value problem*

$$(3.2) \quad \begin{cases} \frac{\partial z}{\partial t} - \operatorname{div}(\alpha \nabla z) = v & \text{in } Q \\ \nu \cdot \alpha \nabla z = 0 & \text{in } \Sigma \\ z(\cdot, 0) = y_0 & \text{in } \Omega \end{cases}$$

belongs to  $W(0, T) \cap \mathcal{C}(\bar{Q})$ . Moreover, the mapping  $v \mapsto z$  is continuous.

The main consequence of Lemma 3.2 is the following result on existence and regularity:

THEOREM 3.3. *Let Assumption 2.1 be satisfied. Then, for every  $u \in \mathbb{R}^n$ , (1.8) admits a unique solution  $(\mathcal{A}, y) \in X \times W(0, T) \cap \mathcal{C}(\bar{Q})$ . The mapping  $u \mapsto (\mathcal{A}, y)$  is continuous from  $\mathbb{R}^n$  to  $X \times W(0, T) \cap \mathcal{C}(\bar{Q})$ .*

*Proof.* We introduce first a sesquilinear form  $a : X \times X \rightarrow \mathbb{C}$  defined by

$$a(\mathcal{A}, \psi) = \int_{\mathcal{D}} (\mu^{-1} \nabla \times \mathcal{A}) \cdot (\nabla \times \bar{\psi}) \, dx + i\omega \int_{\mathcal{I} \cup \Omega} \sigma \mathcal{A} \cdot \bar{\psi} \, dx.$$

Since every vector function from  $X$  is divergence-free, there exists a constant  $c > 0$  depending only on the domain  $\mathcal{D}$  such that

$$\|\psi\|_{L^2(\mathcal{D})^3} \leq c \|\nabla \times \psi\|_{L^2(\mathcal{D})^3} \quad \forall \psi \in X;$$

see [16, Corollary 3.51]. By the latter inequality and (2.1), we have

$$|a(\psi, \psi)| \geq \mu_{\max}^{-1} \int_{\mathcal{D}} (\nabla \times \psi) \cdot (\nabla \times \bar{\psi}) \, dx = \mu_{\max}^{-1} \|\nabla \times \psi\|_{L^2(\mathcal{D}; \mathbb{C})^3}^2 \geq c \|\psi\|_{H(\operatorname{curl}; \mathcal{D})}^2 = c \|\psi\|_X^2 \quad \forall \psi \in X,$$

with a constant  $c > 0$  depending only on  $\mathcal{D}$  and  $\mu_{\max}$ . Thus, the sesquilinear form  $a$  is coercive in  $X$ . Further, by (2.1), it is also clear that  $a$  is bounded. For this reason, the Lax-Milgram lemma implies that the variational problem

$$a(\mathcal{A}, \psi) = F(\psi) \quad \forall \psi \in X$$

admits a unique solution  $\mathcal{A}$  for every  $F \in X^*$ . This guarantees in particular the existence of a unique solution to (3.1a) for every control  $u \in \mathbb{R}^n$ .

Let now  $u \in \mathbb{R}^n$  and  $\mathcal{A} \in X$  be the associated unique solution to (3.1a). Since  $\mathcal{D}$  is convex, the embedding

$$X \hookrightarrow H^1(\mathcal{D}; \mathbb{C})^3$$

holds (see Amrouche et al. [2]) and for this reason

$$\mathcal{A} \in X \longleftrightarrow L^6(\mathcal{D}; \mathbb{C})^3.$$

The latter regularity implies that

$$\frac{\tau\sigma\omega^2}{2} |\mathcal{A}|^2 \in L^3(Q).$$

Then, as  $\Omega \subset \mathcal{D} \subset \mathbb{R}^3$ , Lemma 3.2 yields that (3.1b) admits a unique solution  $y \in W(0, T) \cap \mathcal{C}(\overline{Q})$  and the mapping  $\mathcal{A} \mapsto y$  is continuous from  $X$  to  $W(0, T) \cap \mathcal{C}(\overline{Q})$ . Hence, thanks to the continuity of the mapping  $u \mapsto \mathcal{A}$  from  $\mathbb{R}^n$  to  $X$ , we obtain the continuity of the mapping  $u \mapsto y$ .  $\square$

In what follows, the control-to-state mapping  $u \mapsto y$ , which assigns to every control  $u \in \mathbb{R}^n$  the solution  $y$  of (1.8), is denoted by  $G : \mathbb{R}^n \rightarrow W(0, T) \cap \mathcal{C}(\overline{Q})$ . Using this operator, the optimal control problem (P) can be equivalently written as

$$(P) \quad \begin{cases} \min_{u \in U_{ad}} f(u) := \frac{1}{2} \|E_T G(u) - y_d\|_{L^2(\Omega)}^2 \\ \text{s.t. } G(u)(x, t) \leq y_{\max} \quad \text{for all } (x, t) \in \overline{Q}. \end{cases}$$

Here,  $E_T : W(0, T) \rightarrow L^2(\Omega)$ ,  $y(\cdot) \mapsto y(T)$ , and  $U_{ad} := \{u \in \mathbb{R}^n \mid u_a \leq u_j \leq u_b \ \forall j = 1, \dots, n\}$ . In what follows, a vector  $u \in \mathbb{R}^n$  is said to be a feasible control of (P) if and only if

$$u \in U_{feas} := \left\{ u \in U_{ad} \mid G(u)(x, t) \leq y_{\max} \quad \forall (x, t) \in \overline{Q} \right\}.$$

We assume that  $U_{feas} \neq \emptyset$ . Then, as  $U_{feas}$  is compact and  $f$  is continuous, the Weierstrass theorem implies that (P) admits an optimal solution. Note that the control space is finite-dimensional.

**DEFINITION 3.4.** *Let  $U, Z$  be Banach spaces and let  $Z$  be partially ordered by  $\leq_Z$ . An operator  $F : U \rightarrow Z$  is called convex if*

$$F(su + (1-s)\hat{u}) \leq_Z sF(u) + (1-s)F(\hat{u}) \quad \forall s \in [0, 1], \forall u, \hat{u} \in U.$$

In our case  $U = \mathbb{R}^n$  and  $Z = \mathcal{C}(\overline{Q})$  is partially ordered by its natural ordering  $y \leq_Z 0$  if and only if  $y(x, t) \leq 0$  for all  $(x, t) \in \overline{Q}$ .

**THEOREM 3.5.** *The solution operator  $G : \mathbb{R}^n \rightarrow W(0, T) \cap \mathcal{C}(\overline{Q})$  is convex.*

*Proof.* Let  $\mathcal{A}(u)$  denote the weak solution to (1.8a) for  $u \in \mathbb{R}^n$ . Then, the solution operator  $G$  can also be written as

$$(3.3) \quad G(u) = S \left( \frac{\tau\sigma\omega^2}{2} |\mathcal{A}(u)|^2 \right).$$

Here,  $S : L^r(Q) \rightarrow W(0, T) \cap \mathcal{C}(\overline{Q})$ , with  $r > \frac{3}{2} + 1$ , is a linear bounded operator defined by  $Sv = z$ , where  $z \in W(0, T) \cap \mathcal{C}(\overline{Q})$  is the unique solution of

$$(3.4) \quad \begin{cases} \frac{\partial z}{\partial t} - \operatorname{div}(\alpha \nabla z) = v & \text{in } Q \\ \nu \cdot \alpha \nabla z = 0 & \text{in } \Sigma \\ z(\cdot, 0) = y_0 & \text{in } \Omega; \end{cases}$$

see Lemma 3.2. It is well-known that  $S$  is a nonnegative operator in the following sense:

$$(3.5) \quad v \in L^r(Q) \text{ with } r > \frac{3}{2} + 1 \text{ and } v(x, t) \geq 0 \text{ a.e. in } Q \implies (Sv)(x, t) \geq 0 \quad \forall (x, t) \in \overline{Q}.$$

Notice that  $y_0(x) \geq 0 \forall x \in \Omega$  was postulated in our general assumption (see Assumption 2.1). Therefore, the solution of (3.4) satisfies  $z(x, t) \geq 0$  for all  $(x, t) \in \overline{Q}$ , if the right hand side  $v$  is nonnegative.

As  $u \mapsto \mathcal{A}(u)$  is linear from  $\mathbb{R}^n$  to  $X \hookrightarrow L^6(\mathcal{D}; \mathbb{C})^3$  and thanks to the nonnegativity of the functions  $\tau : [0, T] \rightarrow \mathbb{R}$  and  $\sigma : \mathcal{D} \rightarrow \mathbb{R}$ , the mapping  $u \mapsto \frac{\tau\sigma\omega^2}{2} |\mathcal{A}(u)|^2$  is convex from  $\mathbb{R}^n$  to  $L^3(Q)$ . Let now  $u, \hat{u} \in \mathbb{R}^n$  and  $s \in [0, 1]$ . According to (3.3), we have

$$G(su + (1-s)\hat{u}) = S\left(\frac{\tau\sigma\omega^2}{2} |\mathcal{A}(su + (1-s)\hat{u})|^2\right).$$

By the linearity of  $S$  and the convexity of  $u \mapsto \frac{\tau\sigma\omega^2}{2} |\mathcal{A}(u)|^2$ , it follows from the latter equality that

$$\begin{aligned} G(su + (1-s)\hat{u}) &= sS\left(\frac{\tau\sigma\omega^2}{2} |\mathcal{A}(u)|^2\right) + (1-s)S\left(\frac{\tau\sigma\omega^2}{2} |\mathcal{A}(\hat{u})|^2\right) \\ &\quad + S\left(\underbrace{\frac{\tau\sigma\omega^2}{2} |\mathcal{A}(su + (1-s)\hat{u})|^2 - \left(s\frac{\tau\sigma\omega^2}{2} |\mathcal{A}(u)|^2 + (1-s)\frac{\tau\sigma\omega^2}{2} |\mathcal{A}(\hat{u})|^2\right)}_{\leq 0 \text{ a.e. in } Q}\right) \\ &\leq sS\left(\frac{\tau\sigma\omega^2}{2} |\mathcal{A}(u)|^2\right) + (1-s)S\left(\frac{\tau\sigma\omega^2}{2} |\mathcal{A}(\hat{u})|^2\right) \\ &= sG(u) + (1-s)G(\hat{u}), \end{aligned}$$

where we used (3.5) in the last inequality. In conclusion,  $G : \mathbb{R}^n \rightarrow W(0, T) \cap \mathcal{C}(\overline{Q})$  is convex.  $\square$

An immediate consequence of Theorem 3.5 is the convexity of the feasible set  $U_{feas}$  as we summarize in the following corollary:

**COROLLARY 3.6.** *The feasible set  $U_{feas}$  associated with (P) is convex.*

We should underline that both Theorem 3.5 and Corollary 3.6 do not necessarily imply the convexity of (P). Indeed,  $x^2$  is convex but  $(x^2 - c^2)^2$  for  $c > 0$  is not convex and hence the objective functional  $f : \mathbb{R}^n \rightarrow \mathbb{R}$  is not convex due to the presence of  $y_d$ . For this reason, uniqueness of the optimal solution of (P) cannot be guaranteed. In the sequel, we focus on the analysis of local optima of (P).

**DEFINITION 3.7 (Local optima).** *A feasible control  $u^* \in U_{feas}$  is said to be a local solution to (P) if and only if there exists an  $\epsilon > 0$  such that  $f(u^*) \leq f(u)$  holds true for all feasible controls  $u$  of (P) satisfying  $|u - u^*| < \epsilon$ .*

**3.1. Optimality conditions for (P).** We introduce first the following functions:

**DEFINITION 3.8.**

(i) For  $j = 1, \dots, n$ , let  $\mathcal{A}_j \in X$  be the unique solution of

$$\int_{\mathcal{D}} (\mu^{-1} \nabla \times \mathcal{A}_j) \cdot (\nabla \times \bar{\psi}) dx + i\omega \int_{\mathcal{I} \cup \Omega} \sigma \mathcal{A}_j \cdot \bar{\psi} dx = \int_{\mathcal{I}_j} \mathcal{J}_j \cdot \bar{\psi} dx \quad \forall \psi \in X.$$



(ii) For  $k, l \in \{1, \dots, n\}$ , we define functions  $\mathcal{A}_{k,l}$  by

$$(3.6) \quad \mathcal{A}_{k,l} := \frac{\tau\sigma\omega^2}{2} (\mathcal{R}e(\mathcal{A}_k) \cdot \mathcal{R}e(\mathcal{A}_l) + \mathcal{I}m(\mathcal{A}_k) \cdot \mathcal{I}m(\mathcal{A}_l)),$$

where  $\mathcal{R}e(\mathcal{A}_k)$  and  $\mathcal{I}m(\mathcal{A}_k)$  are the real and imaginary parts of  $\mathcal{A}_k$ , respectively. Note that  $\mathcal{A}_{k,l} \in L^3(Q)$  holds for all  $k, l \in \{1, \dots, n\}$  thanks to the embedding  $X \hookrightarrow L^6(\mathcal{D}; \mathbb{C})^3$ .

We recall that  $\mathcal{A}(u)$  denotes the weak solution to (1.8a) for  $u \in \mathbb{R}^n$ . By the superposition principle,  $\mathcal{A}(u)$  admits the following form:

$$(3.7) \quad \mathcal{A}(u) = \sum_{j=1}^n u_j \mathcal{A}_j \quad \forall u \in \mathbb{R}^n.$$

Thus, the Joule heat source in the right hand side of (3.1b) can be written as

$$(3.8) \quad \begin{aligned} \frac{\tau\sigma\omega^2}{2} |\mathcal{A}(u)|^2 &= \frac{\tau\sigma\omega^2}{2} \left| \sum_{j=1}^n u_j \mathcal{A}_j \right|^2 = \frac{\tau\sigma\omega^2}{2} \sum_{k,l=1}^n u_k u_l (\mathcal{R}e(\mathcal{A}_k) \cdot \mathcal{R}e(\mathcal{A}_l) + \mathcal{I}m(\mathcal{A}_k) \cdot \mathcal{I}m(\mathcal{A}_l)) \\ &\stackrel{(3.6)}{=} \sum_{k,l=1}^n u_k u_l \mathcal{A}_{k,l}. \end{aligned}$$

We define a symmetric  $(n, n)$ -matrix function  $\mathbf{A} : Q \rightarrow \mathbb{R}^{n \times n}$  by

$$(3.9) \quad \mathbf{A}(x, t) = [\mathcal{A}_{k,l}(x, t)].$$

Using this matrix function in (3.8), it follows that

$$(3.10) \quad \frac{\tau\sigma\omega^2}{2} |\mathcal{A}(u)|^2 = u^T \mathbf{A} u,$$

from which we deduce that  $G(u) = y$  is given by the unique solution of

$$(3.11) \quad \begin{cases} \frac{\partial y}{\partial t} - \operatorname{div}(\alpha \nabla y) = u^T \mathbf{A} u & \text{in } Q \\ \nu \cdot \alpha \nabla y = 0 & \text{in } \Sigma \\ y(\cdot, 0) = y_0 & \text{in } \Omega. \end{cases}$$

REMARK 3.9. Notice that the matrix function  $\mathbf{A} : Q \rightarrow \mathbb{R}^{n \times n}$  is positive semidefinite. This follows immediately from (3.10).

The mapping  $u \mapsto u^T \mathbf{A} u$  has the derivative  $2\mathbf{A}u$ . Hence, we obtain for any  $u, h \in \mathbb{R}^n$  that  $z_h = G'(u)h$ , where  $z_h$  solves

$$(3.12) \quad \begin{cases} \frac{\partial z_h}{\partial t} - \operatorname{div}(\alpha \nabla z_h) = 2u^T \mathbf{A} h & \text{in } Q \\ \nu \cdot \alpha \nabla z_h = 0 & \text{in } \Sigma \\ z_h(\cdot, 0) = 0 & \text{in } \Omega. \end{cases}$$

Further, for given  $u \in \mathbb{R}^n$ , the adjoint state  $\varphi \in W(0, T)$  associated with  $u$  is introduced as the unique solution of

$$(3.13) \quad \begin{cases} -\frac{\partial \varphi}{\partial t} - \operatorname{div}(\alpha \nabla \varphi) = 0 & \text{in } Q \\ \nu \cdot \alpha \nabla \varphi = 0 & \text{in } \Sigma \\ \varphi(\cdot, T) = y(\cdot, T) - y_d & \text{in } \Omega, \end{cases}$$

with  $y = G(u)$ . Then, in view of (3.12), the derivative of  $f$  at  $u \in \mathbb{R}^n$  in the direction  $h \in \mathbb{R}^n$  can be expressed as follows:

$$(3.14) \quad f'(u)h = \iint_Q \varphi(x, t) 2u^T \mathbf{A}(x, t) h \, dx dt = \iint_Q \frac{\partial H}{\partial u}(x, t, u, \varphi(x, t)) h \, dx dt.$$

Here, the Hamiltonian  $H : \Omega \times (0, T) \times \mathbb{R}^n \times \mathbb{R} \rightarrow \mathbb{R}$  is defined by

$$H(x, t, u, \varphi) = \varphi u^T \mathbf{A}(x, t) u.$$

To obtain first-order necessary optimality conditions for (P), we assume the existence of an interior (Slater) point with respect to the state constraint (1.9b):

ASSUMPTION 3.10. *Let  $u^* \in U_{feas}$  be a local solution to (P). We assume that there exists a vector  $u_0 \in U_{ad}$  such that*

$$(G(u^*) + G'(u^*)(u_0 - u^*))(x, t) \leq y_{\max} - \epsilon \quad \forall (x, t) \in \overline{Q},$$

with some fixed  $\epsilon > 0$ .

In what follows, Assumption 3.10 is referred to as the *linearized Slater condition*.

THEOREM 3.11. *Let  $u^* \in U_{feas}$  be a local solution to (P) and  $y^* = G(u^*)$ . Suppose that  $u^*$  satisfies the linearized Slater condition. Then, there exist  $\lambda \in \mathcal{M}(\overline{Q})^+$  and  $\varphi^* \in L^\xi((0, T), W^{1,\eta}(\Omega))$  with  $\xi, \eta \in [1, 2)$  and  $2/\xi + 3/\eta > 4$  such that*

$$(3.15a) \quad \begin{cases} -\frac{\partial \varphi^*}{\partial t} - \operatorname{div}(\alpha \nabla \varphi^*) = \lambda|_Q & \text{in } Q \\ \nu \cdot \alpha \nabla \varphi^* = \lambda|_\Sigma & \text{in } \Sigma \\ \varphi^*(\cdot, T) = y^*(\cdot, T) - y_d + \lambda|_{\overline{\Omega} \times \{T\}} & \text{in } \Omega, \end{cases}$$

$$(3.15b) \quad \int_{\overline{Q}} (y^* - y_{\max}) \, d\lambda = 0,$$

$$(3.15c) \quad \iint_Q \frac{\partial H}{\partial u}(x, t, u^*, \varphi^*(x, t))(u - u^*) \, dx dt \geq 0 \quad \forall u \in U_{ad},$$

where  $\lambda_Q$ ,  $\lambda_\Sigma$  and  $\lambda_{\overline{\Omega} \times \{T\}}$  denote the restrictions of  $\lambda$  to the sets  $Q$ ,  $\Sigma$  and  $\overline{\Omega} \times \{T\}$ .

We refer to Casas [6] for the method to prove Theorem 3.11. As a consequence of Theorem 3.11, we obtain a further characterization for the local solution  $u^*$ .

THEOREM 3.12. *Let  $u^* \in U_{feas}$  be a local solution to (P) and  $y^* = G(u^*)$ . Suppose that  $u^*$  satisfies the linearized Slater condition. Then, there exists a pair  $(\lambda, \varphi^*) \in \mathcal{M}(\overline{Q})^+ \times$*

$L^\xi((0, T), W^{1,\eta}(\Omega))$  with  $\xi, \eta \in [1, 2)$  and  $2/\xi + 3/\eta > 4$  satisfying (3.15), and  $u^*$  solves the following linear–quadratic optimization problem:

$$(3.16) \quad \min_{u \in U_{ad}} \frac{1}{2} (\Phi u, u)_{\mathbb{R}^n},$$

where  $\Phi \in \mathbb{R}^{n \times n}$  is a symmetric matrix defined by

$$(3.17) \quad \Phi_{kl} = \iint_Q \varphi^*(x, t) \mathcal{A}_{k,l}(x) dx dt \quad \forall l, k \in \{1, \dots, n\}.$$

*Proof.* Using the symmetric matrix  $\Phi$ , we deduce that

$$(3.18) \quad \begin{aligned} \iint_Q \frac{\partial H}{\partial u}(x, t, u^*, \varphi^*(x, t)) h dx dt &= \iint_Q \varphi^*(x, t) 2u^{*T} \mathbf{A}(x, t) h dx dt \\ &= \iint_Q \varphi^*(x, t) 2 \sum_{k,l=1}^n u_k^* h_l \mathcal{A}_{k,l}(x, t) dx dt \\ &= 2 \sum_{k,l=1}^n u_k^* h_l \iint_Q \varphi^*(x, t) \mathcal{A}_{k,l}(x, t) dx dt \\ &= 2(\Phi u^*, h)_{\mathbb{R}^n} \quad \forall h \in \mathbb{R}^n. \end{aligned}$$

Then, the variational inequality (3.15c) is equivalent to

$$(\Phi u^*, u - u^*)_{\mathbb{R}^n} \geq 0 \quad \forall u \in U_{ad}.$$

The latter variational inequality is exactly the sufficient and necessary optimality condition for the convex optimization problem (3.16). In conclusion, the assertion is valid.  $\square$

Notice that the matrix  $\Phi$  in Theorem 3.12 depends on the adjoint state  $\varphi^*$ . From this theorem, we finally arrive at the following projection formula:

**THEOREM 3.13.** *Let  $u^* \in U_{feas}$  be a local solution to (P) and  $y^* = G(u^*)$ . Suppose that  $u^*$  satisfies the linearized Slater condition. Then, there exists a pair  $(\lambda, \varphi^*) \in \mathcal{M}(\bar{Q})^+ \times L^\xi((0, T), W^{1,\eta}(\Omega))$ , with  $\xi, \eta \in [1, 2)$  and  $2/\xi + 3/\eta > 4$ , satisfying (3.15). For every  $j = 1, \dots, n$ ,  $u_j^*$  obeys the following projection formula:*

$$(3.19a) \quad u_j^* = \mathbb{P}_{[u_a, u_b]} \left( - \sum_{\substack{k=1 \\ k \neq j}}^n \frac{\Phi_{jk}}{\Phi_{jj}} u_k^* \right) \quad \text{if } \Phi_{jj} \neq 0,$$

$$(3.19b) \quad u_j^* = u_a \quad \text{if } \Phi_{jj} = 0 \text{ and } \sum_{k=1}^n \Phi_{jk} u_k^* > 0,$$

$$(3.19c) \quad u_j^* = u_b \quad \text{if } \Phi_{jj} = 0 \text{ and } \sum_{k=1}^n \Phi_{jk} u_k^* < 0,$$

with  $\Phi \in \mathbb{R}^{n \times n}$  defined as in (3.17).

REMARK 3.14. The projection  $\mathbb{P}_{[u_a, u_b]} : \mathbb{R} \rightarrow [u_a, u_b]$  is defined by

$$\mathbb{P}_{[u_a, u_b]}(s) = \begin{cases} u_a & \text{if } s \leq u_a \\ s & \text{if } s \in (u_a, u_b) \\ u_b & \text{if } s \geq u_b. \end{cases}$$

*Proof.* According to Theorem 3.12, we know that

$$(3.20) \quad (\Phi u^*, u - u^*)_{\mathbb{R}^n} \geq 0 \quad \forall u \in U_{ad}.$$

We define a vector  $v \in \mathbb{R}^n$  by

$$v_l = u_l^* \quad \text{for all } l \in \{1, \dots, n\} \setminus \{j\} \quad \text{and} \quad v_j \in [u_a, u_b] \text{ arbitrary.}$$

It is obvious that  $v \in U_{ad}$ . Then, setting  $u = v$  in (3.20) yields

$$(3.21) \quad \left( \sum_{k=1}^n \Phi_{jk} u_k^* \right) (v_j - u_j^*) \geq 0 \quad \forall v_j \in [u_a, u_b],$$

or equivalently

$$(3.22) \quad \left( \sum_{\substack{k=1 \\ k \neq j}}^n \Phi_{jk} u_k^* + \Phi_{jj} u_j^* \right) (v_j - u_j^*) \geq 0 \quad \forall v_j \in [u_a, u_b].$$

Then, if  $\Phi_{jj} \neq 0$ , a standard evaluation of (3.22) implies that

$$u_j^* = \mathbb{P}_{[u_a, u_b]} \left( - \sum_{\substack{k=1 \\ k \neq j}}^n \frac{\Phi_{jk}}{\Phi_{jj}} u_k^* \right).$$

Thus, (3.19a) is valid. Now, if  $\Phi_{jj} = 0$ , then (3.22) gives

$$\left( \sum_{k=1}^n \Phi_{jk} u_k^* \right) (v_j - u_j^*) \geq 0 \quad \forall v_j \in [u_a, u_b],$$

from which we deduce that

$$u_j^* = \begin{cases} u_a & \text{if } \sum_{k=1}^n \Phi_{jk} u_k^* > 0 \\ u_b & \text{if } \sum_{k=1}^n \Phi_{jk} u_k^* < 0. \end{cases}$$

In conclusion, the assertion is valid. □

**4. Reformulation of (P) using the superposition principle.** In the previous section, we have derived optimality conditions for (P) using techniques from the optimal control theory. In the following, we demonstrate that the optimal control problem (P) can be transformed into a (pure) semi-infinite optimization problem *without explicit use of PDEs*. Then, by the theory of semi-infinite programming, we can derive optimality conditions for (P) which do not involve any adjoint state. In addition, we also obtain a more specific structural property for the associated Lagrange multiplier.

DEFINITION 4.1.

(i) For  $k, l \in \{1, \dots, n\}$ , we define  $y_{k,l} \in W(0, T) \cap \mathcal{C}(\bar{Q})$  as the unique solution of

$$\int_0^T \left\langle \frac{\partial y_{k,l}}{\partial t}, \phi \right\rangle_{H^1(\Omega)^*, H^1(\Omega)} dt + \iint_Q \alpha \nabla y_{k,l} \cdot \nabla \phi \, dx dt = \iint_Q \mathcal{A}_{k,l} \phi \, dx dt \quad \forall \phi \in W(0, T),$$

$$y_{k,l}(0) = 0.$$

(ii) Let  $\hat{y} \in W(0, T) \cap \mathcal{C}(\bar{Q})$  be the unique solution of

$$\begin{cases} \frac{\partial \hat{y}}{\partial t} - \operatorname{div}(\alpha \nabla \hat{y}) = 0 & \text{in } Q \\ \nu \cdot \alpha \nabla \hat{y} = 0 & \text{in } \Sigma \\ \hat{y}(\cdot, 0) = y_0 & \text{in } \Omega. \end{cases}$$

Notice that existence and uniqueness of  $y_{k,l} \in W(0, T) \cap \mathcal{C}(\bar{Q})$  and  $\hat{y}$  follows from Theorem 3.3.

LEMMA 4.2. The solution operator  $G : \mathbb{R}^n \rightarrow W(0, T) \cap \mathcal{C}(\bar{Q})$  admits the following decomposition:

$$(4.1) \quad G(u) = \sum_{k,l=1}^n u_k u_l y_{k,l} + \hat{y} \quad \forall u \in \mathbb{R}^n.$$

*Proof.* The assertion follows immediately from (3.11). □

Thanks to (4.1), the optimal control problem (P) can be rephrased as follows:

$$(P) \quad \begin{cases} \min_{u \in U_{ad}} f(u) := \frac{1}{2} \int_{\Omega} \left( \sum_{k,l=1}^n u_k u_l y_{k,l}(x, T) + \hat{y}(x, T) - y_d(x) \right)^2 dx \\ \text{s.t.} \quad \sum_{k,l=1}^n u_k u_l y_{k,l}(x, t) + \hat{y}(x, t) \leq y_{\max} \quad \forall (x, t) \in \bar{Q}. \end{cases}$$

REMARK 4.3. The latter formulation is particularly important for an efficient numerical computation. The functions  $\hat{y}$  and  $y_{k,l}$  for all  $k, l = 1, \dots, n$  are independent of  $u$ . Therefore we only have to compute them once. After determining these quantities, we do not need to solve any PDEs to find an optimal solution to (P).

For a given feasible control  $u \in U_{feas}$ , we define the active set  $\mathcal{F}(u) \subset \bar{Q}$  associated with  $u$  by

$$\mathcal{F}(u) = \left\{ (x, t) \in \bar{Q} \mid \sum_{k,l=1}^n u_k u_l y_{k,l}(x, t) + \hat{y}(x, t) = y_{\max} \right\}.$$

In the upcoming theorem, we state the necessary optimality conditions for (P) obtained from the theory of semi-infinite programming. See the monograph by Bonnans and Shapiro [4, Theorem 4.101]. In what follows, we denote by  $\delta_q$  the Dirac measure concentrated at a point  $q \in \bar{Q}$ .

**THEOREM 4.4.** *Let  $u^* \in U_{feas}$  be a local solution to (P) satisfying the linearized Slater condition and assume that  $\mathcal{F}(u^*) \neq \emptyset$ . Then, there exists  $\lambda = \sum_{j=1}^m \mu_j \delta_{\{(x_j, t_j)\}}$  such that*

$$(4.2a) \quad m \leq n, \quad \mu_1, \dots, \mu_m \geq 0 \quad \text{with} \quad \sum_{j=1}^m \mu_j \neq 0,$$

$$(4.2b) \quad (x_1, t_1), \dots, (x_m, t_m) \in \mathcal{F}(u^*),$$

$$(4.2c) \quad f'(u^*)(u - u^*) + \int_{\bar{Q}} G'(u^*)(u - u^*) d\lambda \geq 0 \quad \forall u \in U_{ad}.$$

Taking now Lemma 4.2 into account, it follows from Theorem 4.4 the following result:

**THEOREM 4.5.** *Let  $u^* \in U_{feas}$  be a local solution to (P) and  $y^* = G(u^*)$ . Assume that  $\mathcal{F}(u^*) \neq \emptyset$  and  $u^*$  satisfies the linearized Slater condition. Then, there exists  $\lambda = \sum_{j=1}^m \mu_j \delta_{\{(x_j, t_j)\}}$  satisfying (4.2), and  $u^*$  solves the following linear-quadratic optimization problem:*

$$\min_{u \in U_{ad}} \frac{1}{2} (Bu, u)_{\mathbb{R}^n},$$

where  $B \in \mathbb{R}^{n \times n}$  is a symmetric matrix defined by

$$(4.3) \quad B_{kl} = \int_{\Omega} (y^*(x, T) - y_d(x)) y_{k,l}(x, T) dx + \sum_{j=1}^m \mu_j y_{k,l}(x_j, t_j) \quad \forall l, k \in \{1, \dots, n\}.$$

*Proof.* As  $y_{k,l} = y_{l,k}$  holds for all  $k, l \in \{1, \dots, n\}$ , (4.1) yields

$$(G'(u^*)h)(x, t) = 2 \sum_{k,l=1}^n u_k^* h_l y_{k,l}(x, t) \quad \forall h \in \mathbb{R}^n, \quad \forall (x, t) \in \bar{Q}.$$

Thus, since  $\lambda = \sum_{j=1}^m \mu_j \delta_{(x_j, t_j)}$ , we deduce that

$$(4.4) \quad \begin{aligned} f'(u^*)h + \int_{\bar{Q}} G'(u^*)h d\lambda &= \int_{\Omega} (y^*(x, T) - y_d(x))(G'(u^*)h)(x, T) dx + \sum_{j=1}^m \mu_j (G'(u^*)h)(x_j, t_j) \\ &= \int_{\Omega} (y^*(x, T) - y_d(x)) \left( 2 \sum_{k,l=1}^n u_k^* h_l y_{k,l}(x, T) \right) dx + \sum_{j=1}^m \mu_j \left( 2 \sum_{k,l=1}^n u_k^* h_l y_{k,l}(x_j, t_j) \right) \\ &= 2 \sum_{k,l=1}^n u_k^* h_l \underbrace{\left( \int_{\Omega} (y^*(x, T) - y_d(x)) y_{k,l}(x, T) dx + \sum_{j=1}^m \mu_j y_{k,l}(x_j, t_j) \right)}_{=B_{kl}} \\ &= 2 (Bu^*, h)_{\mathbb{R}^n}. \end{aligned}$$

For this reason, (4.2c) is equivalent to

$$(4.5) \quad (Bu^*, u - u^*)_{\mathbb{R}^n} \geq 0 \quad \forall u \in U_{ad},$$

from which we deduce that the assertion is valid.  $\square$

**COROLLARY 4.6.** *Let  $u^* \in U_{feas}$  be a local solution to (P) and  $y^* = G(u^*)$ . Assume that  $\mathcal{F}(u^*) \neq \emptyset$  and  $u^*$  satisfies the linearized Slater condition. Then, there exists  $\lambda = \sum_{j=1}^m \mu_j \delta_{\{(x_j, t_j)\}}$  satisfying (4.2). Furthermore, for every  $j = 1, \dots, n$ ,  $u_j^*$  obeys the following projection formula:*

$$(4.6a) \quad u_j^* = \mathbb{P}_{[u_a, u_b]} \left( - \sum_{\substack{k=1 \\ k \neq j}}^n \frac{B_{jk}}{B_{jj}} u_k^* \right) \quad \text{if } B_{jj} \neq 0,$$

$$(4.6b) \quad u_j^* = u_a \quad \text{if } B_{jj} = 0 \text{ and } \sum_{k=1}^n B_{jk} u_k^* > 0,$$

$$(4.6c) \quad u_j^* = u_b \quad \text{if } B_{jj} = 0 \text{ and } \sum_{k=1}^n B_{jk} u_k^* < 0,$$

with  $B \in \mathbb{R}^{n \times n}$  defined as in (4.3).

The proof is completely analogous to the one for Theorem 3.13.

**4.1. Second-order sufficient optimality conditions.** Let us now turn to second-order sufficient optimality conditions for (P). We introduce the cone of critical directions for feasible controls of (P) in the following definition:

**DEFINITION 4.7** (Cone of critical directions). *Let  $u^* \in U_{feas}$  and suppose that  $u^*$  together with  $\lambda = \sum_{j=1}^m \mu_j \delta_{(x_j, t_j)}$  satisfies the first-order optimality system (4.2). Further, let  $B \in \mathbb{R}^{n \times n}$  be defined as in (4.3). We recall from (4.4) that*

$$(4.7) \quad f'(u^*) + \int_{\bar{Q}} G'(u^*) d\lambda = 2Bu^*.$$

(i) *The subset  $\mathcal{C}_{u^*} \subset \mathbb{R}^n$  is defined by  $\mathcal{C}_{u^*} = \{h \in \mathbb{R}^n \mid h \text{ satisfies (4.8) - (4.10)}\}$*

$$(4.8) \quad h_j = \begin{cases} \geq 0 & \text{if } u_j^* = u_a, \\ = 0 & \text{if } (Bu^*)_j \neq 0, \\ \leq 0 & \text{if } u_j^* = u_b, \end{cases}$$

$$(4.9) \quad z_h(x, t) \leq 0 \quad \text{if } y^*(x, t) = y_{\max},$$

$$(4.10) \quad \int_{\bar{Q}} z_h(x, t) d\lambda = 0,$$

where  $z_h = G'(u^*)h = 2 \sum_{k,l=1}^n u_k^* h_l y_{k,l}$ .

(ii) We say that  $u^*$  satisfies the second order sufficient condition (SSC) if

$$(SSC) \quad h^T \frac{\partial^2 \mathcal{L}}{\partial u^2}(u^*, \lambda) h > 0 \quad \forall h \in \mathcal{C}_{u^*} \setminus \{0\},$$

where  $\mathcal{L} : \mathbb{R}^n \times \mathcal{M}(\overline{Q}) \rightarrow \mathbb{R}$  denotes the Lagrangian of (P) defined by

$$\mathcal{L}(u, \lambda) = f(u) + \int_{\overline{Q}} (G(u) - y_{\max}) d\lambda.$$

The upcoming theorem provides a second-order sufficient condition for (P); we refer the reader to [4] for the method of the proof.

**THEOREM 4.8.** *Let  $u^* \in U_{feas}$  and suppose that  $u^*$  together with  $\lambda = \sum_{j=1}^m \mu_j \delta_{(x_j, t_j)}$  satisfies the first-order optimality system (4.2). If  $u^*$  satisfies (SSC), then there exist positive real numbers  $\varepsilon_1$  and  $\varepsilon_2$  such that*

$$f(u^*) + \frac{\varepsilon_2}{2} |u - u^*|_{\mathbb{R}^n} \leq f(u)$$

holds true for every feasible control  $u$  of (P) satisfying  $|u - u^*|_{\mathbb{R}^n} < \varepsilon_1$ . In particular,  $u^*$  is a local solution of (P) according to Definition 3.7.

In general, it is very difficult and even impossible to deduce (SSC) for the continuous problem (P) from those associated with the discretized optimal control problems  $(P_h)$  (see the next section for the details of the discretization). The numerical verification of second order sufficient conditions was investigated by Rösch and Wachsmuth [23]. The analysis is however very technical and only true for a few very special classes of elliptic problems. In our numerical algorithm, we compute the reduced Hessian associated with  $(P_h)$  as an indicator for local optimality of the numerical solution. The Hessian can be easily computed as we only deal with finitely many control parameters. If the Hessian is positive definite, then this is some indication that (SSC) might hold for (P), from which we can expect local optimality. However, this is not a rigorous proof.

**5. Numerical test.** Throughout the experiment, the domain  $\mathcal{D}$  is given by  $(-0.75, 0.75)^3$ . The workpiece  $\Omega$  is located in the center of  $\mathcal{D}$  and is given by a block of height 0.3, width 0.1, and length 0.1. Further, we consider two induction coils  $\mathcal{I}_1$  and  $\mathcal{I}_2$  given by

$$\mathcal{I}_1 = \left\{ \left( \begin{pmatrix} 0 \\ 0 \\ -0.04 \end{pmatrix} + \begin{pmatrix} (0.1 + s \cos \eta) \cos \theta \\ (0.1 + s \cos \eta) \sin \theta \\ s \sin \eta \end{pmatrix} : s \in [0, 0.015], \eta, \theta \in [0, 2\pi] \right\}$$

$$\mathcal{I}_2 = \left\{ \left( \begin{pmatrix} 0 \\ 0 \\ 0.04 \end{pmatrix} + \begin{pmatrix} (0.1 + s \cos \eta) \cos \theta \\ (0.1 + s \cos \eta) \sin \theta \\ s \sin \eta \end{pmatrix} : s \in [0, 0.015], \eta, \theta \in [0, 2\pi] \right\}.$$

Both  $\mathcal{I}_1$  and  $\mathcal{I}_2$  are made of copper (Cu), whereas the workpiece  $\Omega$  is made of silver (Ag). The corresponding material parameters are presented in Table 5.1. The other data used in the numerical test are summarized in the following:

$$T = 360 \text{ (s)}, \quad T_E = 120 \text{ (s)}, \quad y_0 = 293 \text{ (K)}, \quad \omega = 1000 \text{ (Hz)}, \quad u_a = 100 \text{ (V)}, \quad u_b = 1000 \text{ (V)}.$$



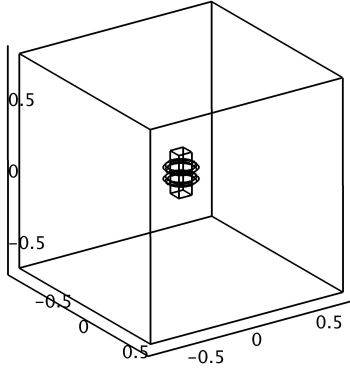


FIG. 5.1. Computational domain  $\mathcal{D}$

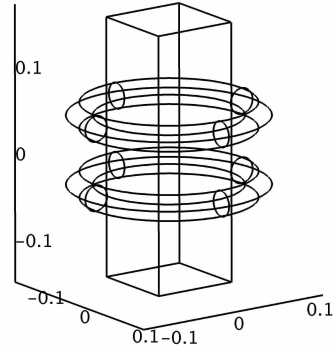


FIG. 5.2. Workpiece  $\Omega$  and coils  $\mathcal{I}_1, \mathcal{I}_2$  inside  $\mathcal{D}$

TABLE 5.1  
Material parameter (left: Cu and right: Ag)

$\mu \left( \frac{\text{H}}{\text{m}} \right)$	$\sigma \left( \frac{\text{S}}{\text{m}} \right)$	$\mu \left( \frac{\text{H}}{\text{m}} \right)$	$\sigma \left( \frac{\text{S}}{\text{m}} \right)$	$\alpha \left( \frac{\text{m}^2}{\text{s}} \right)$
$1,256 \cdot 10^{-6}$	$5.96 \cdot 10^7$	$1.257 \cdot 10^{-6}$	$6.3 \cdot 10^7$	$1.6563 \cdot 10^{-4}$

We recall that the heat source is set to be zero in the time interval  $(T_E, T]$  (see (1.2)). The computational domain  $\bar{\mathcal{D}}$  is divided into a mesh that is refined on the interface  $\partial\Omega$  (see Figures 5.3–5.4). The mesh consists of 30433 tetrahedral, where 13262 tetrahedron are located in  $\bar{\Omega}$ .

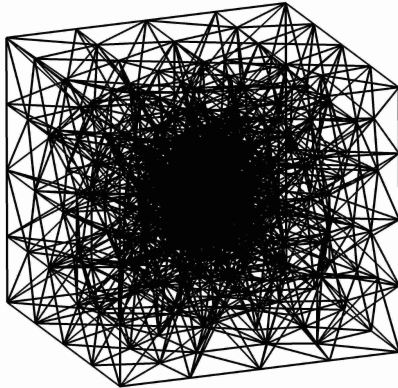


FIG. 5.3. Discretization mesh

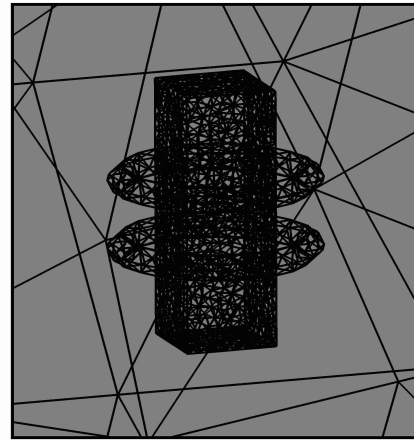


FIG. 5.4. Mesh refinement on  $\partial\Omega$

As we only consider two induction coils and due to our setting, the optimal control problem

(P) becomes

$$(5.1) \quad \begin{cases} \min_{u \in \mathbb{R}^2} \frac{1}{2} \int_{\Omega} (u_1^2 y_{1,1}(x, T) + 2u_1 u_2 y_{1,2}(x, T) + u_2^2 y_{2,2}(x, T) + 293 - y_d(x))^2 dx \\ \text{s.t. } 100 \leq u_1 \leq 1000 \\ \quad 100 \leq u_2 \leq 1000 \\ \quad u_1^2 y_{1,1}(x, t) + 2u_1 u_2 y_{1,2}(x, t) + u_2^2 y_{2,2}(x, t) + 293 \leq y_{\max} \quad \forall (x, t) \in \bar{Q}. \end{cases}$$

To solve (5.1) numerically, we need to determine the functions  $y_{1,1}$ ,  $y_{1,2}$ ,  $y_{2,2}$  (see Definition 4.1) as well as the vector fields  $\mathcal{A}_1$ ,  $\mathcal{A}_2$  (see Definition 3.8). These quantities were numerically computed by the commercial software COMSOL Multiphysics (3D AC/DC Module). More precisely, the variational equalities for  $\mathcal{A}_j$ ,  $j = 1, 2$ , were discretized using second-order Nédélec's curl-conforming edge elements (cf. [17]). Hereafter, the PDEs for the quantities  $y_{1,1}$ ,  $y_{1,2}$ ,  $y_{2,2}$  were discretized using  $\mathbb{P}_1$ -elements (with backward Euler in time).

We denote by  $y_{1,1}^h$ ,  $y_{1,2}^h$ ,  $y_{2,2}^h$  the FEM approximations to  $y_{1,1}$ ,  $y_{1,2}$ ,  $y_{2,2}$ , respectively. As pointed out in Remark 4.3, these FEM approximations have to be solved only once. We found numerically that the mappings

$$t \mapsto \|y_{1,1}^h(\cdot, t)\|_{C(\bar{\Omega})}, \quad t \mapsto \|y_{1,2}^h(\cdot, t)\|_{C(\bar{\Omega})}, \quad t \mapsto \|y_{2,2}^h(\cdot, t)\|_{C(\bar{\Omega})}$$

are monotone increasing in  $[0, T_E]$  and monotone decreasing in  $[T_E, T]$ . For this reason

$$u_1^2 y_{1,1}^h(x, t) + 2u_1 u_2 y_{1,2}^h(x, t) + u_2^2 y_{2,2}^h(x, t) + 293 \leq y_{\max} \quad \forall (x, t) \in \bar{Q}$$

can be equivalently written as

$$u_1^2 y_{1,1}^h(x, T_E) + 2u_1 u_2 y_{1,2}^h(x, T_E) + u_2^2 y_{2,2}^h(x, T_E) + 293 \leq y_{\max} \quad \forall x \in \bar{\Omega},$$

for all  $u_1, u_2 \in \mathbb{R}^+$ . Using the FEM approximations  $y_{1,1}^h$ ,  $y_{1,2}^h$ ,  $y_{2,2}^h$ , we formulate the discrete approximation of the optimization problem (5.1) as follows:

$$(5.2) \quad \begin{cases} \min_{u \in \mathbb{R}^2} f_h(u) := \frac{1}{2} \int_{\Omega} (u_1^2 y_{1,1}^h(x, T) + 2u_1 u_2 y_{1,2}^h(x, T) + u_2^2 y_{2,2}^h(x, T) + 293 - y_d(x))^2 dx \\ \text{s.t. } 100 \leq u_1 \leq 1000 \\ \quad 100 \leq u_2 \leq 1000 \\ \quad u_1^2 y_{1,1}^h(x_j, T_E) + 2u_1 u_2 y_{1,2}^h(x_j, T_E) + u_2^2 y_{2,2}^h(x_j, T_E) + 293 \leq y_{\max} \quad \forall x_j \in \mathcal{N}_h, \end{cases}$$

where  $\mathcal{N}_h \subset \bar{\Omega}$  denotes the set of all nodes of the discretization mesh. In (5.1), the minimizing procedure is restricted to the mesh nodes, as we use  $\mathbb{P}_1$ -elements for the discretization of the temperature. Thus, the extrema are located on the nodes. In general, this is not the case, if we use  $\mathbb{P}_2$ -elements. The problem (5.2) belongs to a class of nonlinear constrained programming problems. We solved it by a quasi-Newton-SQP algorithm (cf. [18, Chapter 8]).

EXAMPLE 5.1. *We choose  $y_d \equiv 500$  and  $y_{\max} = 600$ .*

In Table 5.2, we provide a detailed insight into the convergence behavior of the algorithm for solving Example 5.1. Here  $L$  denotes the Lagrangian associated with the optimization problem (5.2). The algorithm converged to the solution

$$(5.3) \quad u_h = (2.1547566\text{e}+02, 2.1559095\text{e}+02)^T.$$

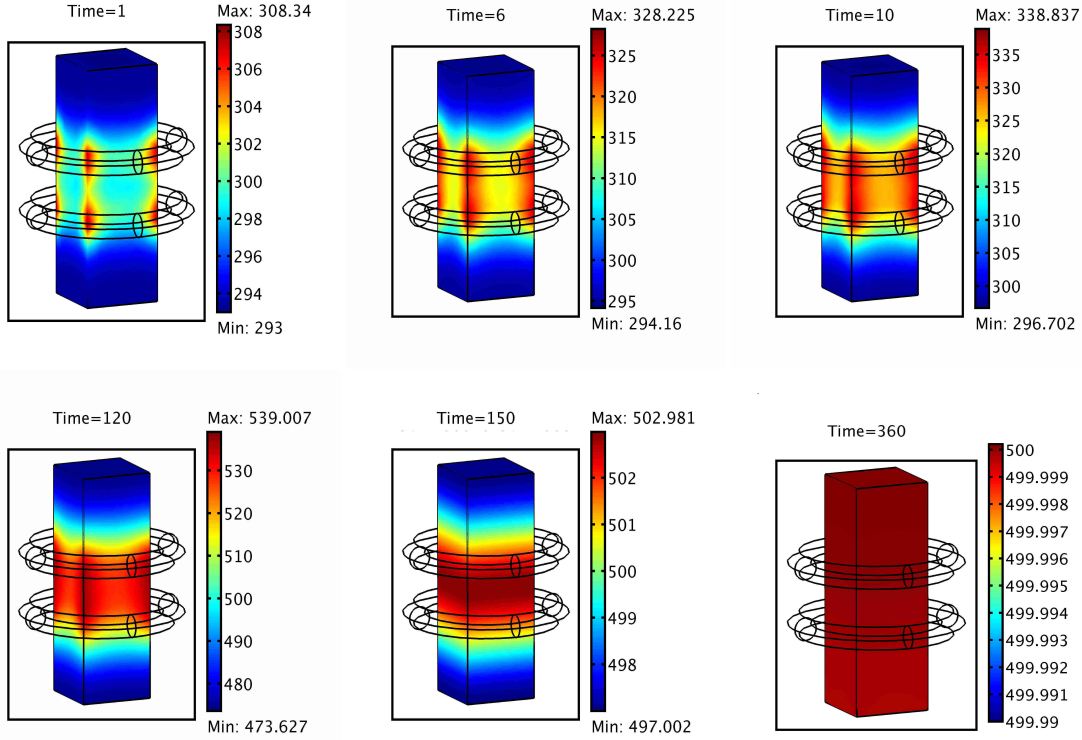


FIG. 5.5. Example 5.1: *optimal temperature  $y_h$  at different times*

In Figure 5.5, we depict the computed optimal temperature  $y_h := u_{h,1}^2 y_{1,1}^h + 2u_{h,1}u_{h,2}y_{1,2}^h + u_{h,2}^2 y_{2,2}^h + 293$ . As visualized in this figure,  $y_h$  does not hit the maximum temperature  $y_{\max}$ , i.e., all inequality constraints at the optimal solution (5.3) are inactive. Hence, Example 5.1 is equivalent to a unconstrained optimization problem. At the final time  $t = T$ , the temperature  $y_h$  approximates the desired temperature  $y_d$  satisfactorily (see Figure 5.5). In fact, the value of the objective functional at the optimal solution is almost zero (see Table 5.2).

TABLE 5.2  
*Convergence history* (Example 5.1)

it.	$f_h(u^k)$	$ \nabla_u L(u^k, \lambda^k) $
1	39.486	0.218
2	7.45342	31.9
3	0.0503673	8.41
4	0.00692233	0.00624
5	3.14349e-06	0.000132
6	3.47882e-10	1.02e-06
7	1.60682e-10	1.26e-09

As mentioned in the previous section, to check (SSC) numerically, we employ the reduced Hessian

$$\nabla_u^2 L(u_h, \lambda_h) = \nabla^2 f_h(u_h) + \sum_{x_j \in \mathcal{N}_h} 2\lambda_{h,j} \begin{pmatrix} y_{1,1}^h(x_j, T_E) & y_{1,2}^h(x_j, T_E) \\ y_{1,2}^h(x_j, T_E) & y_{2,2}^h(x_j, T_E) \end{pmatrix},$$

where  $u_h$  and  $\lambda_h$  are the solution and the Lagrange multiplier computed by our algorithm. In this example,  $u_h$  is given by (5.3) and  $\lambda_h = 0$ . The reduced Hessian computed by our algorithm is given by

$$\begin{pmatrix} 5.0510257e-01 & -4.9675116e-01 \\ -4.9675116e-01 & 4.9947607e-01 \end{pmatrix}.$$

This matrix is positive definite, which indicates that the computed solution (5.3) is a local solution of the continuous problem.

EXAMPLE 5.2. We choose  $y_d \equiv y_{\max} = 500$ .

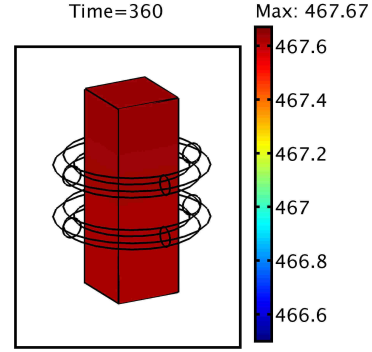
In the second example,  $y_{\max}$  is set to be the same as the desired temperature 500 K. In this case, the algorithm converged to the following solution

$$(5.4) \quad u_h = (1.9650389e+02, 1.9941333e+02)^T.$$

The convergence history of the algorithm is presented in Table 5.3, and we display the computed optimal temperature  $y_h$  at the final time  $t = 360$  in the plot next to Table 5.3.

TABLE 5.3  
Convergence history (Example 5.2)

it.	$f_h(u^k)$	$ \nabla_u L(u^k, \lambda^k) $
1	39.486	0.218
2	8.23604	19.8
3	1.30785	0.523
4	1.60629	0.0166
5	1.60721	0.0159
6	1.57124	0.00354
7	1.57162	6.16e-06
8	1.57162	2.64e-13



Monitoring the above plot, we find that the desired temperature 500 K is not completely achieved (cf. the value of the objective functional in Table 5.3). This is due to the presence of the temperature constraint  $y_h(x, t) \leq y_{\max} = 500$  that has to be satisfied for all  $(x, t) \in \bar{Q}$ . In fact, at the time  $t = T_E$ , the optimal temperature  $y_h$  hits the bound  $y_{\max}$  (cf. Figure 5.6) at the following two nodal points:

$$x^a = (0.05, -0.05, -0.030079)^T, \quad x^b = (0.05, -0.05, 0.01504)^T.$$

In Figure 5.7, we depict the cross sections of  $y_h$  (at  $t = 120$ ) in the  $x_1$ - $x_2$  plane passing through the points  $x^a$  and  $x^b$ , respectively. We monitor that the heat is concentrated at the square edges.

FIG. 5.6. Example 5.2: optimal temperature  $y_h$  at different times

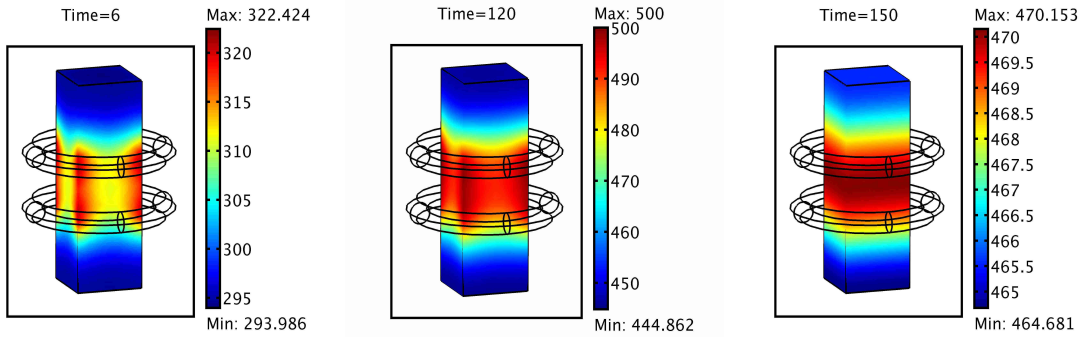
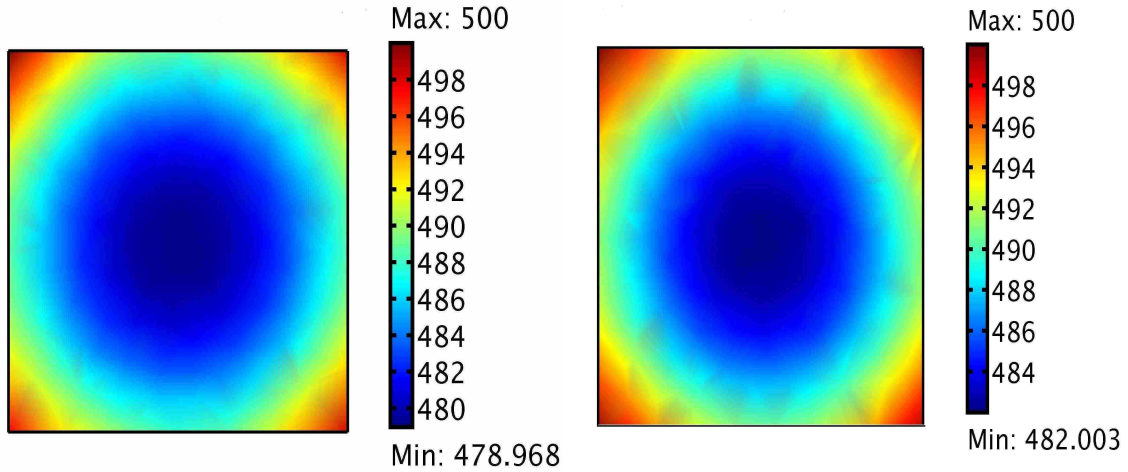


FIG. 5.7. Cross-section of  $y_h$  in the  $x_1$ - $x_2$  plane: left plot  $x_3 = -0.030079$  and right plot  $x_3 = 0.01504$



Further, the heat on the surface of the conductor  $\Omega$  is greater than that in the region around its core. This effect occurs due to the skin effect, well-known for induction heating processes (see [15]).

The computed Lagrange multiplier  $\lambda_h$  associated with the solution (5.4) is positive at the nodal points  $x^a, x^b$  with the values

$$2.8176312e-02, \quad 5.3745619e-02.$$

Then, the approximation to the Lagrange multiplier for the undiscretized problem (5.1) is given by

$$\lambda = \mu_1 \delta_{(x^a, T_E)} + \mu_2 \delta_{(x^b, T_E)},$$

with  $\mu_1 := 2.8176312e-02$  and  $\mu_2 := 5.3745619e-02$ . Finally, as in the previous example, the reduced

Hessian for Example 5.2 is positive definite:

$$\begin{pmatrix} 2.3406088e - 03 & 2.3187394e - 03 \\ 2.3187394e - 03 & 2.3740902e - 03 \end{pmatrix}.$$

This provides an indication for local optimality of the computed solution (5.4).

#### REFERENCES

- [1] A. Alonso and A. Valli. *Eddy Current Approximation of Maxwell Equations: Theory, Algorithms and Applications*. Springer, 2010.
- [2] C. Amrouche, C. Bernardi, M. Dauge, and V. Girault. Vector potentials in three-dimensional non-smooth domains. *Mathematical Methods in the Applied Sciences*, 21:823–864, June 1998.
- [3] O. Bodart, A.V. Boureau, and R. Touzani. Numerical investigation of optimal control of induction heating processes. *Applied Mathematical Modelling*, 25(8):697 – 712, 2001.
- [4] F. Bonnans and A. Shapiro. *Perturbation Analysis of Optimization Problems*. Springer-Verlag, New York, 2000.
- [5] A. Bossavit and J.-F. Rodrigues. On the electromagnetic induction heating problem in bounded domains. *Adv. Math. Sci. Appl.*, 4:79–92, 1994.
- [6] E. Casas. Pontryagin’s principle for state-constrained boundary control problems of semilinear parabolic equations. *SIAM J. Control and Optimization*, 35:1297–1327, 1997.
- [7] S. Clain, J. Rappaz, M. Swierkosz, and Touzani R. Numerical modelling of induction heating for two-dimensional geometries. *M<sup>3</sup>AS*, 3:805–7822, 1993.
- [8] S. Clain and R. Touzani. A two-dimensional stationary induction heating problem. *Mathematical Methods in the Applied Sciences*, 20:759–766, 1997.
- [9] P.-E. Druet, O. Klein, Sprekels J., F. Tröltzsch, and I. Yousept. Optimal control of three-dimensional state-constrained induction heating problems with nonlocal radiation effects. *SIAM J. on Control and Optimization*, 49:1707–1736, 2011.
- [10] J. A. Griepentrog. Maximal regularity for nonsmooth parabolic problems in Sobolev-Morrey spaces. *Adv. Differential Equations*, 12(9):1031–1078, 2007.
- [11] P. Grisvard. *Elliptic Problems in Nonsmooth Domains*. Pitman, Boston, 1985.
- [12] D. Hömberg. *Induction hardening of steel – modeling, analysis and optimal design of inductors*. Habilitation thesis, TU Berlin, 2001.
- [13] D. Hömberg. A mathematical model for induction hardening including mechanical effects. *Nonlinear Anal. Real World Appl.*, 5:55–90, 2004.
- [14] J. L. Lions and E. Magenes. *Problèmes aux limites non homogènes et applications*, volume 1–3. Dunod, Paris, 1968.
- [15] A. C. Metaxas. *Foundations of Electroheat : A Unified Approach*. Wiley, 1996.
- [16] P. Monk. *Finite element methods for Maxwell’s equations*. Clarendon press, Oxford, 2003.
- [17] J.C. Nédélec. Mixed finite elements in  $\mathbb{R}^3$ . *Numer. Math.*, 35:315–341, 1980.
- [18] J. Nocedal and S. J. Wright. *Numerical Optimization*. Springer-Verlag, New York, 1999.
- [19] C. Parietti and J. Rappaz. A quasi-static two-dimensional induction heating problem. I: Modelling and analysis. *Mathematical Models & Methods in Applied Sciences*, 8(6):1003–1021, 1998.
- [20] C. Parietti and J. Rappaz. A quasi-static two-dimensional induction heating problem II. numerical analysis. *Mathematical Models & Methods in Applied Sciences*, 9(9):1333–1350, 1999.
- [21] J. Rappaz and M Swierkosz. Mathematical modelling and numerical simulation of induction heating processes. *Appl. Math. Comput. Sci.*, 6:207–221, 1996.
- [22] F. Tröltzsch. *Optimal control of partial differential equations*, volume 112 of *Graduate Studies in Mathematics*. American Mathematical Society, Providence, RI, 2010.
- [23] D. Wachsmuth and A. Röscher. How to check numerically the sufficient optimality conditions for infinite-dimensional optimization problems. In *Optimal control of coupled systems of partial differential equations*, volume 158 of *Internat. Ser. Numer. Math.*, pages 297–317. Birkhäuser Verlag, Basel, 2009.
- [24] I. Yousept. Optimal control of a nonlinear coupled electromagnetic induction heating system with pointwise state constraints. *Mathematics and its Applications/ Annals of AOSR*, 2(1):45–77, 2010.
- [25] I. Yousept. Optimal control of Maxwell’s equations with regularized state constraints. *Computational Optimization and Applications*, 2011. DOI: 10.1007/s10589-011-9422-2.